Bioresource Technology 261 (2018) 10–18

Contents lists available at ScienceDirect

Bioresource Technology

journal homepage: www.elsevier.com/locate/biortech

Multivariate relationships between microbial communities and environmental variables during co-composting of sewage sludge and agricultural waste in the presence of PVP-AgNPs

Lihua Zhang[a,b], Jiachao Zhang[c], Guangming Zeng[a,b,*], Haoran Dong[a,b], Yaoning Chen[a,b], Chao Huang[d], Yuan Zhu[a,b], Rui Xu[a,b], Yujun Cheng[a,b], Kunjie Hou[a,b], Weicheng Cao[a,b], Wei Fang[a,b]

[a] College of Environmental Science and Engineering, Hunan University, Changsha 410082, PR China
[b] Key Laboratory of Environmental Biology and Pollution Control, Hunan University, Ministry of Education, Changsha 410082, PR China
[c] College of Resources and Environment, Hunan Agricultural University, Changsha 410082, PR China
[d] College of Environmental Science and Engineering, Central South University of Forestry and Technology, Changsha 410004, PR China

GRAPHICAL ABSTRACT

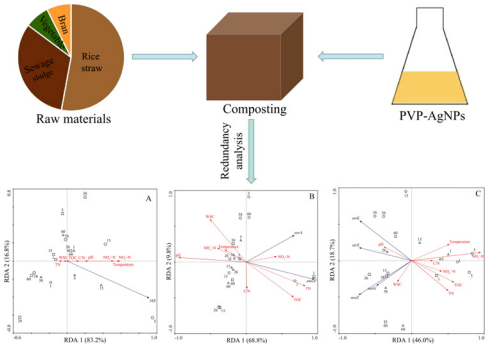

ARTICLE INFO

Keywords:
Co-composting
PVP-AgNPs
16S rDNA
Nitrogen functional genes
Redundancy analysis

ABSTRACT

This study evaluated the contributions of environmental variables to the variations in bacterial 16S rDNA, nitrifying and denitrifying genes abundances during composting in the presence of polyvinylpyrrolidone coated silver nanoparticles (PVP-AgNPs). Manual forward selection in redundancy analysis (RDA) indicated that the variation in 16S rDNA was significantly explained by NO_3^--N, while nitrifying genes were significantly related with pH, and denitrifying genes were driven by NO_3^--N and TN. Partial RDA further revealed that NO_3^--N solely explained 28.8% of the variation in 16S rDNA abundance, and pH accounted for 61.8% of the variation in nitrifying genes. NO_3^--N and TN accounted for 34.2% and 9.2% of denitrifying genes variation, respectively. The RDA triplots showed that different genes shared different relationships with environmental parameters. Based on these findings, a composting with high efficiency and quality may be conducted in the future work by adjusting the significant environmental variables.

* Corresponding author at: College of Environmental Science and Engineering, Hunan University, Changsha 410082, PR China.
E-mail address: zgming@hnu.edu.cn (G. Zeng).

https://doi.org/10.1016/j.biortech.2018.03.089
Received 30 January 2018; Received in revised form 14 March 2018; Accepted 17 March 2018
Available online 29 March 2018
0960-8524/

1. Introduction

Nanoparticles, which have a great ratio of surface area to volume, are defined as particles having at least one dimension with size ranging from 1 to 100 nm (Feng et al., 2013). With the distinctive physico-chemical properties and rapid development of nanotechnology, the engineered nanoparticles (ENPs) were widely used in consumer products and industries. It has been summarized that more than 1800 types of consumer goods contained ENPs (Setyawati et al., 2015). And the ENPs are always applied to the improvement of soil, water and air quality, and to improve the qualities and properties of consumer products (Michels et al., 2017). Silver nanoparticles (AgNPs), as one of the fastest growing and largest portions in commercial ENPs market (Xu et al., 2012a), are widely used in many consumer products such as food containers, food supplements, medical, laundry additives, paints, home appliances and fabrics (Das et al., 2012; Ren et al., 2018; Wu et al., 2017). In addition, AgNPs are prevalent in some industrial fields for their unique physico-chemical properties including catalytic activity, chemical stability and effective conductivity (Zhang et al., 2016a). With the expanding use of AgNPs, the corresponding release into the environment is inevitable. Some studies have reported that AgNPs are easily released from the AgNPs containing products, such as clothes and exterior wall paints, and about 34–80% of Ag are released in the form of AgNPs (Geranio et al., 2009; Gong et al., 2009). It was once investigated that the annual release of AgNPs to wastewater from clothes and washing systems has reached up to 270 tonnes (Blaser et al., 2008). Many of the released AgNPs will enter into the wastewater treatment plants (WWTP) with wastewater. A research performed by United States Environmental Protection Agency (USEPA) suggested that the concentration of Ag in sewage sludge (SS) was in the range of 1.94–856 mg/kg dry sludge, of which about 73% was in the range of 1–20 mg/kg (Tang et al., 2014). Another study about the production of biosolids from 1950 to 2009 in U.S.A, U.K. and Australia indicated that the Ag concentration was in the range between 4.3 and 332 mg/kg and higher concentration was found in the older biosolids (Donner et al., 2015; Long et al., 2011). As about 50% of SS is recycled as soil conditioner and agricultural fertilizer, AgNPs are also very likely to enter into the terrestrial environment. And the concentration of AgNPs in soil has been predicted from 0.02 μg/kg to 4.4 mg/kg (Chen et al., 2015; Cheng et al., 2016).

It was once found that AgNPs could influence the bacterial community of forest soil in terms of both quantity and quality by selecting the insusceptible microbes (Carbone et al., 2014; Zhang et al., 2015a). A previous literature by Liang et al. (2010) demonstrated that nitrifying bacteria was more vulnerable to AgNPs than Ag^+, and the microbial community structures of ammonium-oxidizing bacteria and nitrite-oxidizing bacteria, *Nitrospira* were decreased after the shock load of AgNPs, and the nitrite-oxidizing bacteria, *Nitrobacter* was absolutely washed out. Das et al. (2012) also found that the exposure to AgNPs resulted in changes of bacterioplankton community structures in natural waters. However, the impacts of AgNPs are reported to be associated with environmental factors (Xu et al., 2012b). For instance, it was reported that the antimicrobial ability of AgNPs was weakened in the saline estuarine water environment (Bradford et al., 2009; Deng et al., 2013), while another literature showed that AgNPs significantly affected the microbial community structure in the activated sludge (Alito and Gunsch, 2014). Many researches also have indicated that environmental factors (temperature, pH, moisture and climate, etc.) can affect bacterial or fungal community abundance and structure, and these factors can interact with each other (Buyer et al., 2010; Liang et al., 2017). Guo et al. (2013) also found that soil physico-chemical properties significantly explained the variations of abundance and structure of denitrifying genes, and each of these parameters showed different contributions to the variation of denitrifying genes. However, few literatures studied the influence of environmental variables on the variation of microbes with the existence of AgNPs.

Generally, the abundances of *amoA* and *nxrA* genes involved in ammonia oxidation and nitrite oxidation, respectively, were regarded as the nitrifers abundances, and *narG*, *nirK*, *nirS* and *nosZ* involved in nitrate reduction, nitrite reduction and nitrous oxide reduction, respectively, were considered as denitrifiers. The present work aimed to study the dynamics of the abundances of bacterial, nitrifying and denitrifying genes during composting in the presence of AgNPs, and to investigate the contributions of environmental variables to changes of these microbial communities. Polyvinylpyrrolidone coated AgNPs (PVP-AgNPs) were introduced for the stability under the condition of high ionic strength (Zhang et al., 2017). The physico-chemical parameters in each pile were measured. Quantitative PCR (qPCR) was performed to determine the abundances of bacterial and nitrogen functional genes. Multivariate analysis was conducted to clarify the relationship between physico-chemical parameters and the abundances of bacterial, nitrifying and denitrifying genes. The sole explanation of each significant factor was calculated using partial redundancy analysis (RDA).

2. Materials and methods

2.1. PVP-AgNPs synthesis and characterization

The PVP-AgNPs were synthesized as described in our previous study (Zhang et al., 2017). Firstly, $NaBH_4$ was dissolved in 1% PVP solution to obtain a concentration of 2.5×10^{-3} M. Then, 5×10^{-3} M $AgNO_3$ solutions were dropped into the above solutions with a burette and the final volume ratio was 1:3. The whole process was conducted with a continuous and vigorous stir in the condition of ice bath. One kDa dialysis bags were used to purify the synthesized AgNPs by removing the remaining reactants and the concentrations were remained the same since the redundant by-products were replaced by water.

UV-vis absorption spectrum between wavelength of 300–800 nm was obtained using Shimadzu UV-2550 (Japan) to verify the formation of AgNPs. Then, the morphology and size of PVP-AgNPs were investigated using transmission electron microscopy (TEM) by JEOL, JEM-2100F equipped with energy dispersive X-ray spectroscopy (EDX).

2.2. Composting setup and sampling

The collection and pretreatment of composting materials were described in our previous study (Zhang et al., 2017). Chamber composting piles in 65 L boxes (0.54 m × 0.39 m × 0.31 m, length × width × height) containing rice straw, sewage sludge, bran and vegetable at a weight ratio of 36:22:5:5 were conducted. The physico-chemical characterizations of raw materials were displayed in Table 1. The initial C/N and moisture content were adjusted to about 25 and 65%, respectively. Five treatments were conducted as follows: pile 1 was the control without PVP-AgNPs, and pile 2-pile 5 was added with 2, 10, 20, 30 mg/kg compost of PVP-AgNPs, respectively. The piles were turned daily during the first 2 weeks and weekly afterwards to ensure enough

Table 1
The physico-chemical parameters in raw composting materials.

Materials	Moisture content (%)	pH	TN (g kg^{-1})	TOC (g kg^{-1})	C/N
Sewage sludge	9.48	6.74	24.2	178.9	7.4
Rice straw	10.35	n.d.	10.3	488.9	47.5
Bran	14.62	n.d	21.0	528.2	21.0
Vegetable	94.84	n.d.	22.8	446.4	22.8

The data was presented based on dry weight of the raw composting materials.
n.d., not determined.
TN, total nitrogen.
TOC, total organic carbon.
C/N, TOC/TN.

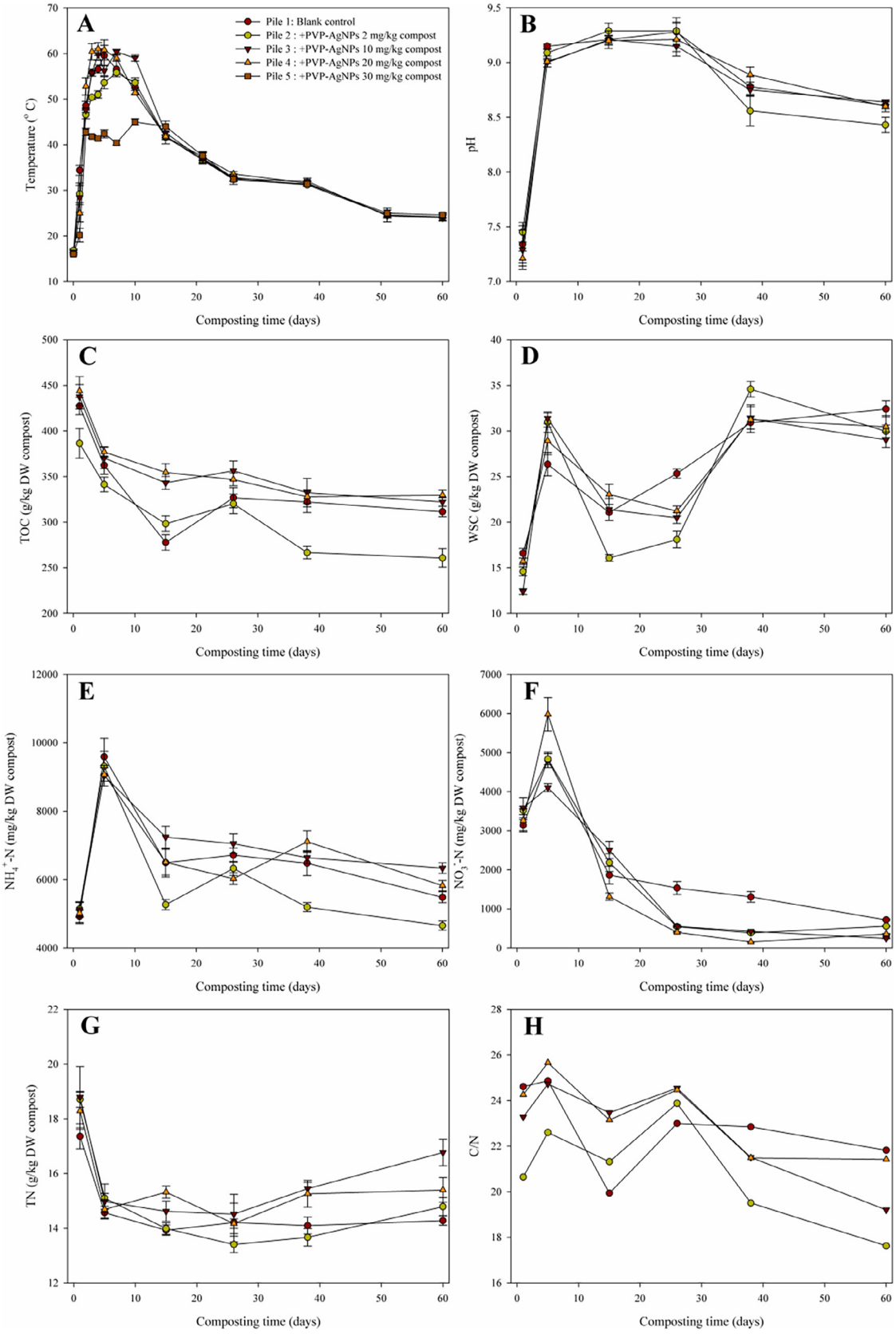

Fig. 1. Time courses of physico-chemical parameters during co-composting: (A) Temperature; (B) pH; (C) TOC; (D) WSC; (E) NH_4^+-N; (F) NO_3^--N; (G) TN; (H) C/N. Mean values and standard deviations (the bars, $n = 5$ for temperature, $n = 3$ for other parameters) are shown. Data are presented on a dry-weight compost basis.

oxygen. Samples were collected on day 1, 5, 15, 26, 38, 60, respectively. One part of the samples was stored at 4 °C before analyses of physico-chemical parameters, and the other part was saved at −20 °C for genomic DNA extraction.

2.3. Determination of physico-chemical parameters

The temperature was recorded using precise thermometers. Samples for determinations of pH and water soluble organic carbon (WSC) were firstly shaken with ultrapure water at a ratio of 1:10 (w/v) for 1 h at 200 rpm, and then the suspension was filtered using filter paper for determination by digital pH meter. The filtrate needed a further centrifugation at 12,000 rpm for about 10 min and a successive filtration using 0.45 μm filter membrane for WSC determination by Total Organic Carbon Analyzer (TOC-5000A, Shimadzu, Japan). The concentration of total organic carbon (TOC) was calculated with reference to the following equation (Zhang et al., 2017):

$$\%TOC = (100-\%ash)/1.8 \quad (1)$$

in which the ash content was determined by dry combustion of the samples for 6 h at 550 °C and the samples were dried for 24 h at 105 °C and grounded beforehand. Samples for determinations of NH_4^+-N and NO_3^--N were shaken in 2 M KCl solution at a ratio of 1:50 (w/v) for 1 h at 150 rpm. Then the solution was filtered using filter paper and centrifuged for 10 min at 5000 rpm. Afterthat, the supernatant was cleared using 0.45 μm filter membrane. Kjeldahl digestion was conducted to measure the total nitrogen (TN) after the sample was dried for 24 h at 105 °C and grounded. C/N amounted to the ratio of TOC and TN.

2.4. DNA extraction

Triplicate extractions of the total genomic DNA was performed by using the E.Z.N.A. ®Soil DNA Kit (OMEGA Bio-Tek, Inc., Norcross, GA, USA) following the manufacturer's instructions. Then the crude DNA was purified using DNA Purification Kit (TIANGEN, China). NanoDrop (Thermo Scientific, Wilmington, DE, USA) was used to determine the concentration and quality of the purified DNA.

2.5. qPCR of bacterial 16S rDNA and nitrogen functional genes

The qPCR reaction of 16S rDNA, nitrifying and denitrifying genes was conducted on the iCycler IQ5 Thermocycler (Bio-Rad, USA) in a 20 μL reaction system consisting of 0.4 μL of the each primer, 10 μL of 2 × SuperRedal PreMix Plus, 1 μL of DNA extraction, and 8.2 μL of sterile ultrapure water. The primers and protocols for amplification were shown in Supplementary materials. Negative controls were set up by replacing the DNA samples with sterile ultrapure water. The unit of gene abundances was expressed as copies/g dry weight (DW) compost.

2.6. Statistical analysis

The temperature was determined in five different locations, and other parameters were determined in triplicate. Mean values and standard deviations were shown in the present study. The differences between mean values were evaluated by least significant difference (LSD) test using SPSS (version 19.0). Canoco 4.5 was used to determine the multivariate relationships between 16S rDNA, nitrifying genes, denitrifying genes and physico-chemical parameters. The longest gradient of all axes determined by detrended correspondence analysis (DCA) was < 3, which indicated that linear model was more suitable for 16S rDNA, nitrifying genes, denitrifying genes. Hence, RDA with Monte Carlo permutation test (499 unrestricted permutations) was conducted to link the changes of microbial community with environmental variables. Manual forward selection was used to test which variables could significantly explain the changes of these microbial genes. Partial RDA was used to determine the single contribution of each significant variable.

3. Results and discussion

3.1. Characterization of PVP-AgNPs

The characterizations of PVP-AgNPs were shown in Supplementary Materials. The UV-vis spectrum showed a peak at around 400 nm and this confirmed that the synthesis of PVP-AgNPs was successful in the present study. The morphology of the prepared AgNPs was almost spherical with average size of 6 nm. The results of EDX about the black spots in the TEM picture further verified the formation of AgNPs.

3.2. Changes of physico-chemical parameters during composting

Temperature is deemed as a vital indicator of microbial activity and organic matter decomposition during composting (Huang et al., 2017). In this study, the highest temperature in pile 5 was lower than 50 °C (Fig. 1A), which did not meet the demand of Chinese National Standard that the temperature should maintain higher than 50 °C for 5 days at least and the minimum standard that the temperature should be higher than 55 °C for 3 days to kill the pathogens during composting (Wan et al., 2017; Zhang et al., 2011). This might be due to that the activity of microbes was strictly inhibited by AgNPs at a concentration of 30 mg/kg to produce enough heat. Therefore, other parameters in pile 5 were not discussed any more in the following contents. In the other four piles, the temperature was divided into three representative stages, including mesophilic, thermophilic and cooling phase. The degradation of some simple organic matters resulted in the rapid rise of temperatures during the first few days. It was fastest to reach the highest temperature for pile 4 on day 4 (61 °C), while pile 1 on day 5 (59.6 °C), pile 2 and 3 on day 7 (55.8 and 60.4 °C, respectively), and the thermophilic phase lasted for 11 days in pile 4 and 10 days in other three piles. The higher temperature peak and longer thermophilic stage in pile 4 were possibly induced by the emergence of microbial species which were tolerant to AgNPs and the small competition for nutrition on account of the damage of other vulnerable species. Previous studies found that the microbial growth was stimulated after short-term exposure to 124 and 287 mg Ag/kg soil comparing with 49 mg Ag/kg soil (Samarajeewa et al., 2017). As shown in Fig. 1B, pH values in all piles increased quickly during the first 5 days and slowly during day 5 to day 26. Previous studies suggested that the production of NH_4^+-N by ammonification of organic nitrogen was conducive to the rise of pH (Huang et al., 2017; Tan et al., 2015). Due to the losses of NH_4^+-N as NH_3 and the generation of organic acids which were the byproducts of organic matter decomposition, pH decreased slowly after day 26.

Utilized by microbes as the energy sources, TOC concentration decreased dramatically at the initial phase of composting (0–15 days) (Fig. 1C) since the decomposition of some easily biodegradable organic matters (OM) by microorganisms. Nakhshiniev et al. (2014) pointed that a part of the organic carbon was decomposed into H_2O, CO_2 and energy, and the remaining part was decomposed into stable humus like substances during the early phase of composting. With completion of simple OM decomposition, the remaining OM mainly composed of lignin and cellulose was difficult to degrade, which slowed down the loss of TOC during cooling and maturation stages. After 60 days of composting process, 27.08%, 32.53%, 26.35%, 25.69% of the initial TOC were degraded in pile1, pile2, pile 3 and pile 4, respectively. Stamou et al. (2016) found that the carbon mineralization was higher with higher AgNPs exposure and the reason was that higher AgNPs would inhibit the generation of humins which could slow down the OM mineralization. While in the present study, the degradation of TOC was the highest in pile 2 which was treated with PVP-AgNPs at a concentration of 2 mg/kg compost, and it decreased with higher AgNPs concentration, this might be due to that the activity of microbial degradation of TOC was inhibited by higher concentration of AgNPs. The

WSC concentrations of all piles increased quickly within the beginning 5 days followed by decreasing and increasing again (Fig. 1D), similar to other studies (Zhang et al., 2016b), since the WSC concentration would increase due to the solubilization of simple organic compounds and WSC might be secreted by microbes or microbial growth during composting which was also a synthesis process. While the WSC decreased sequentially as it was utilized to support microbial population when decomposing the recalcitrant matters. The average concentrations of WSC in pile 1–4 were as follows: 25.45, 24.05, 24.35, and 25.11 g/kg DW compost, respectively. These results indicated that the treatment with AgNPs at a concentration of 2 mg/kg compost promoted the degradation of TOC, thereby needing to consume more WSC which was easily degraded to maintain the microbial population.

The concentration of NH_4^+-N increased rapidly during the first 5 days (Fig. 1E), indicating the ammonification of organic nitrogen. Then it decreased rapidly during the following 10 days as the high temperature and pH was in favor of emission of NH_3, and immobilization of NH_4^+-N by nitrogen fixing microorganisms (Wang et al., 2016b; Zhou et al., 2018). On the basis of the whole composting process, the NH_4^+-N concentration in pile 3 was higher than the other piles, indicating that the addition of AgNPs at a concentration of 10 mg/kg compost promoted the conservation of inorganic N. NO_3^--N was relatively lower than NH_4^+-N (Fig. 1F) which was in accordance with the previous literature (Wang et al., 2013). TN concentrations of all piles decreased rapidly during the first 5 days and slowly between 5 and 26 days due to the emission of NH_3 (Fig. 1G). Subsequently, the TN concentrations gradually increased as the degradation of organic carbonaceous compounds. At the end of composting, the highest level of TN was observed in pile 3, indicating that the treatment with AgNPs at a concentration of 10 mg/kg compost was conducive to the retention of TN. The differences of nitrogen transformation might be induced by the control of nitrogen-transformation functional enzymes and genes by AgNPs (Zeng et al., 2018).

C/N ratio is widely used as the indicator of compost maturity. A satisfactory composting requires that C/N ratio should be < 25 (Chan et al., 2016). The C/N ratio in all piles showed a similar variation trend with an increase during the early 5 days due to the rapid loss of TN through NH_3 release and then a decrease on the whole (Fig. 1H). The decrease of C/N ratio might be attributed to the degradation of OM which could lead to CO_2 release and C/N decline (Zhang et al., 2017).

3.3. Bacterial 16S rDNA and nitrogen functional genes abundances

The copy numbers of bacterial and nitrogen functional genes were quantified by qPCR. As shown in Fig. 2, the bacterial 16S rDNA gene abundance in all treatments increased in the first 5 days, and decreased afterwards with an increase again after 38 days except pile 4 which decreased continuously. The average abundance was 1.14×10^{12}, 1.49×10^{12}, 1.06×10^{12}, 4.84×10^{11} copies/g dry weight (DW) compost in pile 1, pile 2, pile 3 and pile 4, respectively. This was consistent with other previous studies which demonstrated that the higher concentration of AgNPs induced lower soil bacterial abundance and the possible reason was that more Ag element entered into microbial cells and the microbial metabolism was inhibited under higher concentrations of AgNPs (He et al., 2016).

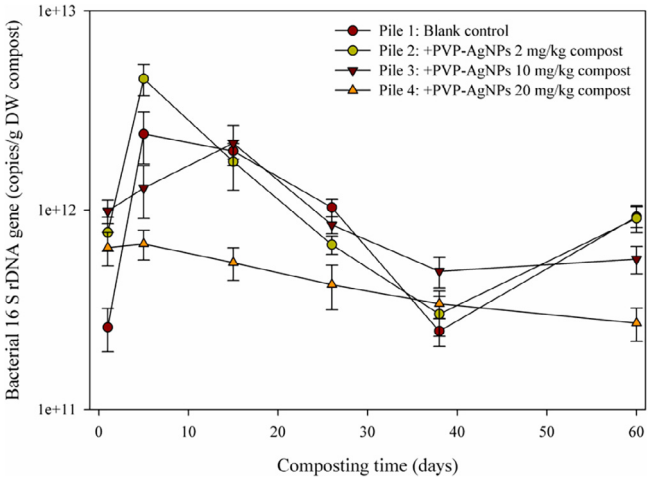

Fig. 2. Changes of bacterial 16S rDNA gene abundance during co-composting. Mean values and standard deviations (the bars, $n = 3$) are shown.

The changes of nitrification functional genes (*amoA* and *nxrA*) abundances were presented in Fig. 3A and B. A decrease of *amoA* gene abundance was observed during the whole composting process in all piles. Averagely, the highest abundance level of 3.15×10^6 copies/g DW compost was achieved in pile 4 which was treated with AgNPs at a concentration of 20 mg/kg compost, while it was 3.13×10^6, 2.67×10^6, 2.62×10^6 copies/g DW compost in pile 1, pile 2 and pile 3, respectively. This finding suggested that AgNPs at a concentration of lower than10 mg/kg compost had a detrimental impact on bacterial *amoA* and it might stimulate *amoA* when the concentration was 20 mg/kg compost during the composting process. Previous literatures have also demonstrated the sensitivity of bacterial *amoA* gene to AgNPs (Beddow et al., 2017; Liang et al., 2010), while they also found that archaea *amoA* gene abundance was not significantly affected. *NxrA* gene, the marker of oxidation of NO_2^--N to NO_3^--N, was also sensitive to AgNPs during the composting process. The average *nxrA* gene copy number was 5.70×10^6, 4.02×10^6, 2.63×10^6, 2.94×10^6 copies/g DW compost in pile 1, pile 2, pile 3, and pile 4, respectively. Liang et al. (2010) once found that the population of the dominant nitrite-oxidizing bacteria genus *Nitrospira* in activated sludge was reduced after a shock load of AgNPs and the genus *Nitrobacter* was not detected.

Fig. 4A–D showed the changes of *narG*, *nirK*, *nirS* and *nosZ*, respectively. In terms of *narG*, pile 1 and pile 2 presented similar trends with a gradual increase and reached peak values on day 38, while pile 3 and pile 4 showed similar trends with a decrease in the first 5 days and then an increase till day 26 followed by a decrease afterwards. *NirK* and *nirS* both participated in the reduction of NO_2^--N to NO which is the first step of gas emission during denitrification. In the present study, the average abundance of *nirK* in each pile was higher than that of *nirS*, suggesting that *nirS* gene was more susceptible to AgNPs and *nirK* gene was the more important contributor to production of NO during the nitrite reduction step (Wang et al., 2016a). The order of average abundance of *nirK* and *nirS* in all piles was pile 2 (9.68×10^9 copies/g DW compost) > pile 1 (7.08×10^9 copies/g DW compost) > pile 4 (6.77×10^9 copies/g DW compost) > pile 3 (3.19×10^9 copies/g DW compost) and pile 2 (2.48×10^9 copies/g DW compost) > pile 4 (2.19×10^9 copies/g DW compost) > pile 3 (2.18×10^9 copies/g DW compost) > pile 1 (1.98×10^9 copies/g DW compost), respectively. These results indicated that the treatment with AgNPs at a concentration of 10 mg/kg could reduce the NO emission. A previous research also demonstrated oscillations of *nirS* and *nirK* after the bacteria was exposed to AgNPs (Guilger et al., 2017). *NosZ* can encode the N_2O reductase to transform N_2O into N_2 which can reduce the emission of greenhouse gas and the environmental pollution. As shown in Fig. 4D, the copy number of *nosZ* in each pile fluctuated differently under different concentrations of AgNPs along with the composting process. In general, the order of average abundance in all piles was pile 4 (1.78×10^8 copies/g DW compost) > pile 3 (1.65×10^8 copies/g DW compost) > pile 2 (1.10×10^8 copies/g DW compost) > pile 1 (5.32×10^7 copies/g DW compost). Other literatures found that the *nosZ* abundance increased in the first two periods (15 and 30 days) after exposed to AgNPs and decreased in the last two periods (90 and 180 days), and their results also indicated the *nosZ* abundance was higher in the treatment with higher concentration of AgNPs in the period of 30 days (Guilger et al., 2017).

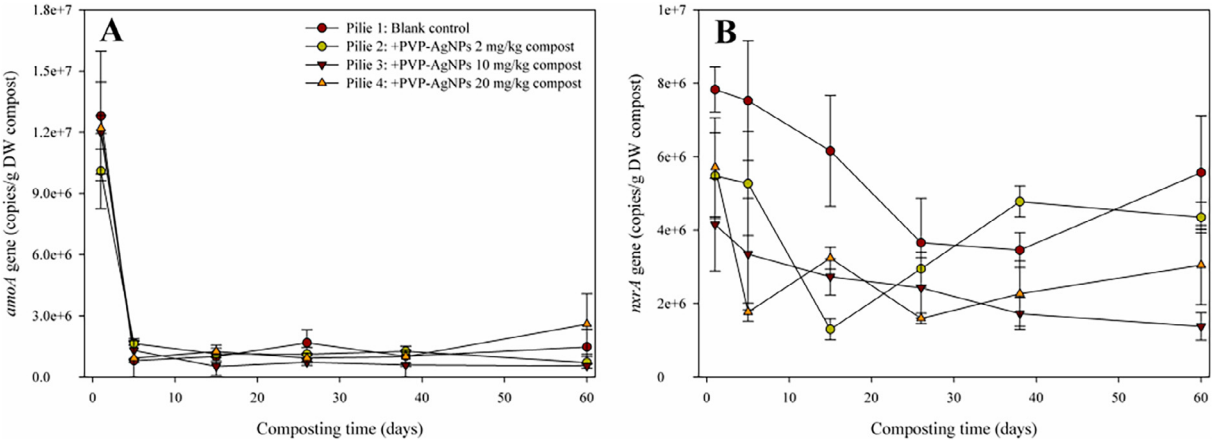

Fig. 3. Changes of nitrifying genes abundances during co-composting: (A) *amoA* gene; (B) *nxrA* gene. Mean values and standard deviations (the bars, $n = 3$) are shown.

3.4. Contributions of environmental variables to bacterial 16S rDNA and nitrogen functional genes abundance

To make certain which of physico-chemical parameters would be the driving factors of the variations, RDA between genes abundances and environmental variables, including temperature, WSC, TOC, NO_3^--N, NH_4^+-N, TN, C/N, and pH, were conducted (see Supplementary materials). The results of Monte-Carlo test with 499 permutations suggested that the relationships between the three categories of genes and environmental variables were statistically significant on both of the first canonical axis and total canonical axes ($P < 0.05$). The first axis explained 83.2%, 68.8%, 46.0% of the variance in 16S rDNA, nitrifying, and denitrifying genes abundances, respectively, and the second axis explained the variance by 16.8%, 9.8%, 18.7%, respectively. Manual forward selection was conducted to identify the significant gradients which drove the succession of microbial abundances. Consequently, the distribution of 16S rDNA gene abundance was significantly influenced by NO_3^--N ($P < 0.05$). While pH ($P < 0.01$) was the only significant factor for the variation of nitrifying genes, and the key factors for variation of denitrifying genes were NO_3^--N ($P < 0.01$) and TN ($P < 0.05$). Partial RDA was used to calculate the single contribution of each significant factor without influences of other factors. The results (Table 2) indicated that NO_3^--N solely explained 28.8% ($P = 0.012$) of the variation in 16S rDNA gene abundance. It was pointed out that pH

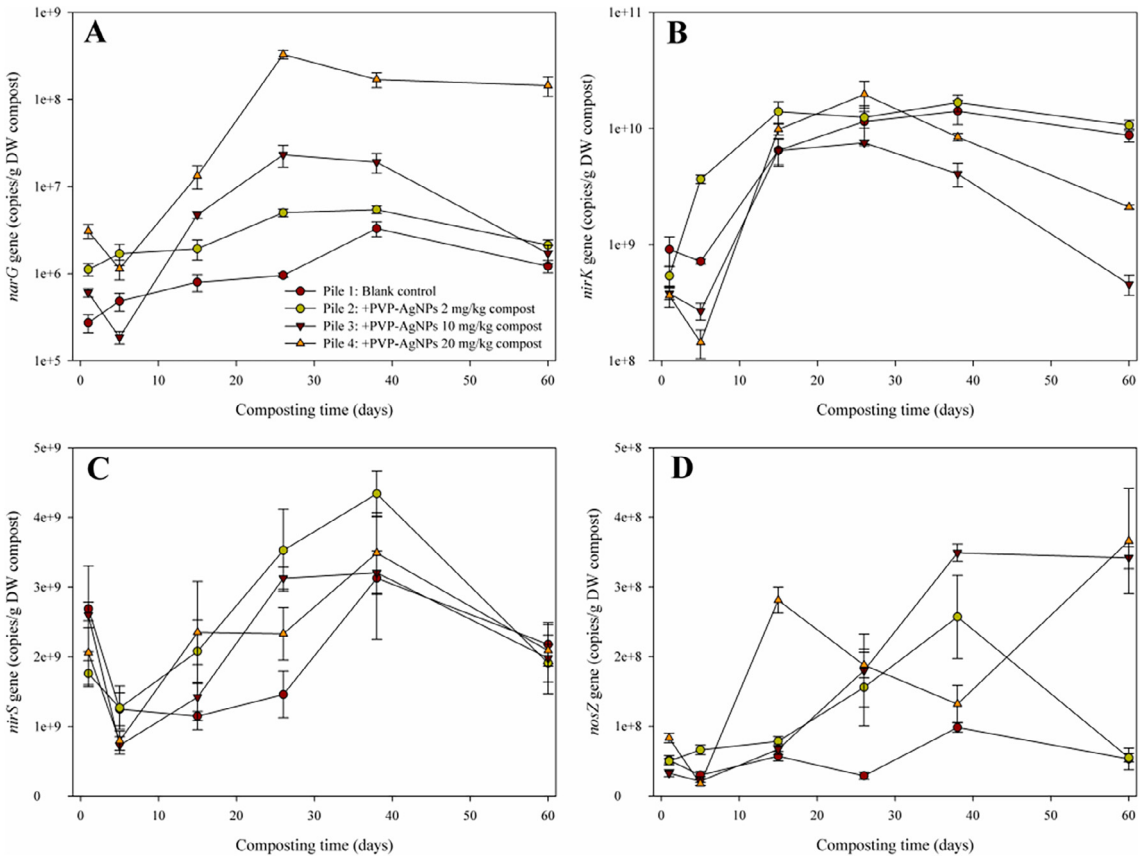

Fig. 4. Changes of denitrifying genes abundances during co-composting: (A) *narG* gene; (B) *nirK* gene; (C) *nirS* gene; (D) *nosZ* gene. Mean values and standard deviations (the bars, $n = 3$) are shown.

Table 2
Results of partial RDA testing the influence of the significant environmental variables on the genes abundances.

Genes	Environmental factors included in partial RDA	Eigenvalues	Solely explained (%)	*F* value	*P* value
16S rDNA	NO_3^--N	0.288	28.8	6.468	0.012
Nitrifying genes	pH	0.618	61.8	25.877	0.002
Denitrifying genes	NO_3^--N	0.342	34.2	10.489	0.002
	TN	0.092	9.2	2.812	0.026
	All the above together	0.511	51.1	7.849	0.002

acted as a selective driver in soil microbes and had a universal impact on the abundance of bacteria (Bru et al., 2011). In the present study, pH solely explained 61.8% ($P = 0.002$) of the variance in nitrifying community abundance. As a typical parameter affecting microbial metabolism and growth, pH was also found to be significantly ($P < 0.01$) correlated with the abundances of nitrifying genes in soil (Lu et al., 2017). Serving as the electron acceptor in the denitrification process, the reduction of NO_3^--N is the first step during this process. Previous studies demonstrated that NO_3^--N concentration was one of the factors shaping denitrifiers (Jones et al., 2010). Similarly, NO_3^--N was the most significant factor with a single explanation of 34.2% ($P = 0.002$) of the variation in denitrifiers abundance in the present study. However, some other previous studies revealed that NO_2^--N shared a stronger relationship than NO_3^--N with denitrifying community, indicating that the reduction of NO_3^--N might be a rate-limiting step during denitrification (Guo et al., 2013). Another significant factor TN solely accounted for 9.2% ($P = 0.026$) and the shared contribution of the two significant factors selected in manual forward selection was 7.7%, indicating that the inter-correlation of significant factors was also influential to the succession of denitrifying genes. The importance of TN in shaping denitrifying community composition and abundance has been also demonstrated by the previous study (Ligi et al., 2014). However, it did not imply that other parameters were not important to the variation in abundances of microbes, since the total explanation of all variables (83.2%, $P = 0.018$, $F = 5.557$; 78.5%, $P = 0.004$, $F = 4.118$; 73.4%, $P = 0.008$, $F = 3.104$ for 16S rDNA, nitrifying genes and denitrifying genes, respectively) were greater than the contributions of significant parameters. It could be only deduced that other environmental variables also contributed to the changes of microbial communities although the significance level was relatively low ($P > 0.05$), as also proposed by Huang et al. (2017).

To evaluate the relationship between 16S rDNA, nitrogen functional genes and environmental variables, ordination triplot was generated after RDA analysis to show the distribution of microbial abundance along with environmental variables. The angle between two angles < 90° represents a positive relationship, and the smaller angle implies a stronger positive relationship. In contrast, the angle more than 90° indicates a negative relationship, and the greater angle also implies a stronger negative relationship. Additionally, the arrow length reflects the importance of the parameter, and the orientation represents the association between the parameter and axis. As shown in Fig. 5A, the variation of 16S rDNA gene abundance was explained by all the parameters on the first axis and it was most positively correlated with NO_3^--N. While the two kinds of nitrifying genes *amoA* and *nxrA* shared a negative relationship with pH (Fig. 5B). As the range of pH was more than 7, it was indicated that the neutral and slight alkali environment might be more favorable for the growth of nitrifiers. Furthermore, the nitrifying genes were also negatively correlated with WSC, NH_4^+-N and temperature, and positively correlated with TN, TOC and NO_3^--N. Differently, *nxrA* was negatively related with C/N, while positive correlation was found between *amoA* and C/N. As presented in Fig. 5C, all

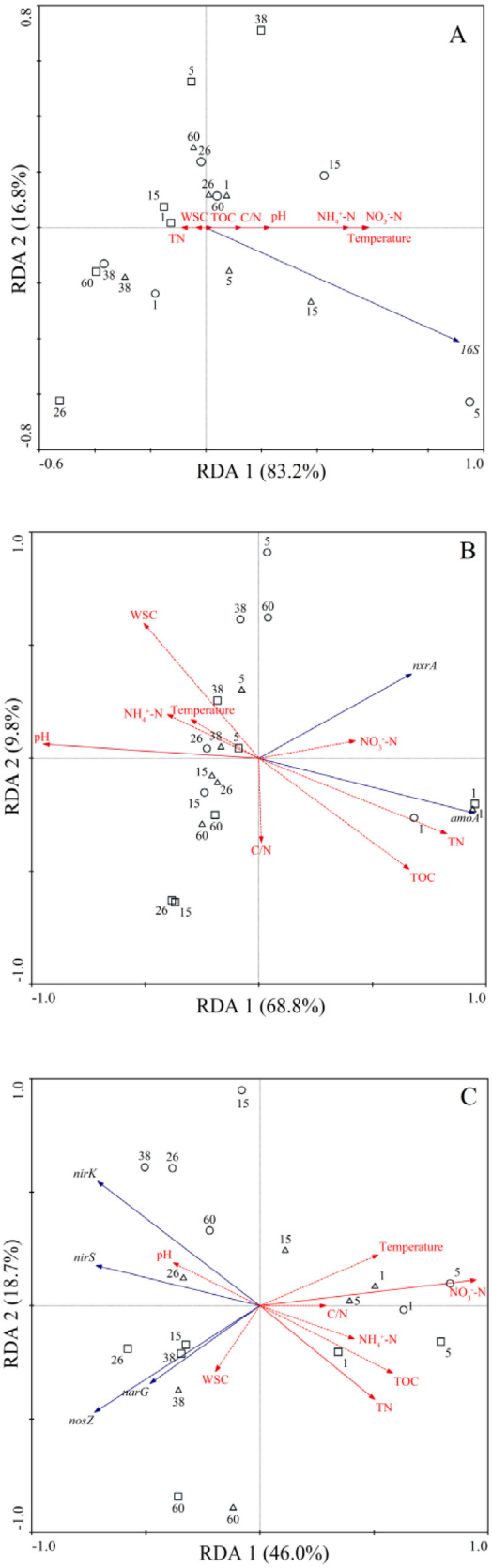

Fig. 5. RDA triplot: (A) 16S rDNA; (B) nitrifying genes; (C) denitrifying genes. Significant variables are indicated by red-solid lines. While supplementary variables are indicated by red-dotted lines. Microbial genes are showed by blue-solid lines. Samples are represented by *circles* (Pile 2), *up-triangles* (Pile 3), and *squares* (Pile 4). The numbers around sample symbols represent the sampling days.

the denitrifying genes were negatively correlated with all the selected parameters (especially NO_3^--N and TN), except pH and WSC. Microorganisms are the main drivers of organic matters decomposition during composting and previous studies have demonstrated that the dynamics of microbes are influenced by environmental conditions greatly (Wang et al., 2017). It was also demonstrated that physico-chemical parameters could influence the abundance of bacterial, nitrifying or denitrifying communities (Huang et al., 2017; Zhang et al., 2015b; Guo et al., 2013). Understanding the relationship between physico-chemical parameters and microbes, and finding the main influential factors could be an effective method to control the microbial communities and hence improve the composting process. Further work is needed to study the diversity of microbial communities and look for the main species during composting treated with AgNPs, and further explore the association between species and environmental parameters. This will help us conduct a more effective composting process by controlling the significantly influential factors.

4. Conclusions

This study investigated the relationship between variations in 16S rDNA, nitrifying genes, denitrifying genes abundances and physico-chemical parameters, respectively, during composting in the presence of AgNPs. The variance of 16S rDNA gene abundance was significantly explained by NO_3^--N, while the variances in nitrifying genes abundances were significantly related with pH and the variations of denitrifying genes abundances showed significant positive relationship with NO_3^--N and TN. The variation in each kind of gene abundance showed different associations with parameters, providing strategies to improve the composting and reduce the loss of nitrogen by controlling the relevant environmental parameters of composting.

Acknowledgments

This study was financially supported by the National Natural Science Foundation of China, China (51521006, 51378190, 51409100, 51408219) and the Program for Changjiang Scholars and Innovative Research Team in University (IRT-13R17).

Appendix A. Supplementary data

Supplementary data associated with this article can be found, in the online version, at https://doi.org/10.1016/j.biortech.2018.03.089.

References

Alito, C.L., Gunsch, C.K., 2014. Assessing the effects of silver nanoparticles on biological nutrient removal in bench-scale activated sludge sequencing batch reactors. Environ. Sci. Technol. 48, 970–976.
Beddow, J., Stolpe, B., Cole, P.A., Lead, J.R., Sapp, M., Lyons, B.P., Colbeck, L., Whitby, C., 2017. Nanosilver inhibits nitrification and reduces ammonia-oxidizing bacterial but not archaeal *amoA* gene abundance in estuarine sediments. Environ. Microbiol. 19, 500–510.
Blaser, S.A., Scheringer, M., Macleod, M., Hungerbuhler, K., 2008. Estimation of cumulative aquatic exposure and risk due to silver: contribution of nano-functionalized plastics and textiles. Sci. Total Environ. 390, 396–409.
Bradford, A., Handy, R.D., Readman, J.W., Atfield, A., Muhling, M., 2009. Impact of silver nanoparticles contamination on the genetic diversity of natural bacterial assemblages in estuarine sediments. Environ. Sci. Technol. 43, 4530–4536.
Bru, D., Ramette, A., Saby, N.P.A., Dequiedt, S., Ranjard, L., Jolivert, C., Arrouays, D., Philippot, L., 2011. Determinants of the distribution of nitrogen-cycling microbial communities at the landscape scale. ISME J. 5, 532–542.
Buyer, J.S., Teasdale, J.R., Roberts, D.P., Zasada, I.A., Maul, J.E., 2010. Factors affecting soil microbial community structure in tomato cropping systems. Soil Biol. Biochem. 42, 831–841.
Carbone, S., Antisari, L.V., Gaggia, F., Baffoni, L., Gioia, D.D., Vianello, G., Nannipieri, P., 2014. Bioavailability and biological effect of engineered silver nanoparticles in a forest soil. J. Hazard. Mater. 280, 89–96.
Chan, M.T., Selvam, A., Wong, J.W.C., 2016. Reducing nitrogen loss and salinity during 'struvite' food waste composting by zeolite amendment. Bioresource Technol. 200, 838–844.
Chen, M., Xu, P., Zeng, G.M., Yang, C.P., Huang, D.L., Zhang, J.C., 2015. Bioremediation of soils contaminated with polycyclic aromatic hydrocarbons, petroleum, pesticides, chlorophenols and heavy metals by composting: applications, microbes and future research needs. Biotechnol. Adv. 33, 745–755.
Cheng, M., Zeng, G.M., Huang, D.L., Lai, C., Xu, P., Zhang, C., Liu, Y., 2016. Hydroxyl radicals based advanced oxidation processes (AOPs) for remediation of soils contaminated with organic compounds: a review. Chem. Eng. J. 284, 582–598.
Das, P., Williams, C.J., Fulthorpe, R.R., Hoque, M.E., Metcalfe, C.D., Xenopoulos, M.A., 2012. Changes in bacterial community structure after exposure to silver nanoparticles in natural waters. Environ. Sci. Technol. 46, 9120–9128.
Deng, J.H., Zhang, X.R., Zeng, G.M., Gong, J.L., Niu, Q.Y., Liang, J., 2013. Simultaneous removal of Cd (II) and ionic dyes from aqueous solution using magnetic graphene oxide nanocomposite as an adsorbent. Chem. Eng. J. 226, 189–200.
Donner, E., Scheckel, K., Sekine, R., Popelka-Filcoff, R., Bennett, J., Brunetti, G., Naidu, R., McGrath, S., Lombi, E., 2015. Non-labile silver species in biosolids remain stable throughout 50 years of weathering and ageing. Environ. Pollut. 205, 78–86.
Feng, Y.Z., Cui, X.C., He, S.Y., Dong, G., Chen, M., Wang, J.H., Lin, X.G., 2013. The role of metal nanoparticles in influencing arbuscular mycorrhizal fungi effects on plant growth. Environ. Sci. Technol. 47, 9496–9504.
Geranio, L., Heuberger, M., Nowack, B., 2009. The behavior of silver nanotextiles during Washing. Environ. Sci. Technol. 43, 8113–8118.
Gong, J.L., Wang, B., Zeng, G.M., Yang, C.P., Niu, C.G., Niu, Q.Y., Zhou, W.J., Liang, Y., 2009. Removal of cationic dyes from aqueous solution using magnetic multi-wall carbon nanotube nanocomposite as adsorbent. J. Hazard. Mater. 164, 1517–1522.
Guilger, M., Pasquoto-Stigliani, T., Bilesky-Jose, N., Grillo, R., Abhilash, P.C., Fraceto, L.F., de Lima, R., 2017. Biogenic silver nanoparticles based on *trichoderma harzianum*: synthesis, characterization, toxicity evaluation and biological activity. Sci. Rep. 7, 44421.
Guo, G.X., Deng, H., Qiao, M., Yao, H.Y., Zhu, Y.G., 2013. Effect of long-term wastewater irragation on potential denitrification and denitrifying communities in soils at the watershed scale. Environ. Sci. Technol. 47, 3105–3113.
He, S.Y., Feng, Y.Z., Ni, J., Sun, Y.F., Xue, L.H., Feng, Y.F., Yu, Y.L., Lin, X.G., Yang, L.Z., 2016. Different responses of soil microbial metabolic activity to silver and iron oxide nanoparticles. Chemosphere 147, 195–202.
Huang, C., Zeng, G.M., Huang, D.L., Lai, C., Xu, P., Zhang, C., Cheng, M., Wan, J., Hu, L., Zhang, Y., 2017. Effect of *Phanerochaete chrysosporium* inoculation on bacterial community and metal stabilization in lead-contaminated agricultural waste composting. Bioresour. Technol. 243, 294–303.
Jones, C.M., Hallin, S., 2010. Ecological and evolutionary factors underlying global and local assembly of denitrifier communities. ISME J. 4, 633–641.
Liang, J., Yang, Z.X., Tang, L., Zeng, G.M., Yu, M., Li, X.D., Wu, H.P., Qian, Y.Y., Li, X.M., Luo, Y., 2017. Changes in heavy metal mobility and availability from contaminated wetland soil remediated with combined biochar-compost. Chemosphere 181, 281–288.
Liang, Z.H., Das, A., Hu, Z.Q., 2010. Bacterial response to a shock load of nanosilver in an activated sludge treatment system. Water Res. 44, 5432–5438.
Ligi, T., Truu, M., Truu, J., Nõlvak, H., Kaasik, A., Mitsch, W.J., Mander, Ü., 2014. Effects of soil chemical characteristics and water regime on denitrification genes (*nirS*, *nirK*, and *nosZ*) abundances in a created riverine wetland complex. Ecol. Eng. 72, 47–55.
Long, F., Gong, J.L., Zeng, G.M., Chen, L., Wang, X.Y., Deng, J.H., Niu, Q.Y., Zhang, H.Y., Zhang, X.R., 2011. Removal of phosphate from aqueous solution by magnetic Fe-Zr binary oxide. Chem. Eng. J. 171, 448–455.
Lu, X.M., Zhen, P., Yang, K., 2017. Restoration using *Azolla imbricata* increases nitrogen functional bacterial groups and genes in soil. Appl. Microbiol. Biot. 101, 3849–3859.
Michels, C., Perazzoli, S., Soares, H.M., 2017. Inhibition of an enriched culture of ammonia oxidizing bacteria by two different nanoparticles: silver and magnetite. Sci. Total Environ. 586, 995–1102.
Nakhshiniev, B., Biddinika, M.K., Gonzales, H.B., Sumida, H., Yoshikawa, K., 2014. Evaluation of hydrothermal treatment in enhancing rice straw compost stability and maturity. Bioresour. Technol. 151, 306–313.
Ren, X.Y., Zeng, G.M., Tang, L., Wang, J.J., Wan, J., Liu, Y.N., Yu, J.F., Yi, H., Ye, S.J., Deng, R., 2018. Sorption, transport and biodegradation-an insight into bioavailability of persistent organic pollutants in soil. Sci. Total Environ. 610–611, 1154–1163.
Samarajeewa, A.D., Velicogna, J.R., Princz, J.I., Subasinghe, R.M., Scroggins, R.P., Beaudette, L.A., 2017. Effect of silver nano-particles on soil microbial growth, activity and community diversity in a sandy loam soil. Environ. Pollut. 220, 504–513.
Setyawati, M.L., Tay, C.Y., Leong, D.T., 2015. Mechanistic investigation of the biological effects of SiO_2, TiO_2, and ZnO nanoparticles on intestinal cells. Small 11, 3458–3468.
Stamou, L., Antizar-Ladislao, B., 2016. The impact of silver and titanium dioxide nanoparticles on the in-vessel composting of municipal solid waste. Waste Manage. 56, 71–78.
Tan, X.F., Liu, Y.G., Zeng, G.M., Wang, X., Hu, X.J., Gu, Y.L., Yang, Z.Z., 2015. Application of biochar for the removal of pollutants from aqueous solutions. Chemosphere 125, 70–85.
Tang, W.W., Zeng, G.M., Gong, J.L., Liang, J., Xu, P., Zhang, C., Huang, B.B., 2014. Impact of humic/fulvic acid on the removal of heavy metals from aqueous solutions using nanomaterials: a review. Sci. Total Environ. 468–469, 1014–1027.
Wan, J., Zeng, G.M., Huang, D.L., Hu, L., Xu, P., Huang, C., Deng, R., Xue, W.J., Lai, C., Zhou, C.Y., Zheng, K.X., Ren, X.Y., Gong, X.M., 2017. Rhamnolipid stabilized nanochlorapatite: synthesis and enhancement effect on Pb- and Cd- immobilization in polluted sediment. J. Hazard. Mater. 343, 332–339.
Wang, C., Lu, H.H., Dong, D., Deng, H., Strong, P.J., Wang, H.L., Wu, W.X., 2013. Insight into the effects of biochar on manure composting: evidence supporting the relationship between N_2O emission and denitrifying community. Environ. Sci. Technol. 47, 7341–7349.
Wang, H.L., Ji, G.D., Bai, X.Y., 2016a. Distribution patterns of nitrogen micro-cycle

functional genes and their quantitative coupling relationships with nitrogen transformation rates in a biotrickling filter. Bioresour. Technol. 209, 100–107.
Wang, Q., Wang, Z., Awasthi, M.K., Jiang, Y.H., Li, R.H., Ren, X.N., Zhao, J.C., Shen, F., Wang, M.J., Zhang, Z.Q., 2016b. Evaluation of medical stone amendment for the reduction of nitrogen loss and bioavailability of heavy metals during pig manure composting. Bioresour. Technol. 220, 297–304.
Wang, X.Q., Cui, H.Y., Shi, J.H., Zhao, X.Y., Zhao, Y., Wei, Z.M., 2017. Relationship between bacterial diversity and environmental parameters during composting of different raw materials. Bioresour. Technol. 243, 294–303.
Wu, H.P., Lai, C., Zeng, G.M., Liang, J., Chen, J., Xu, J.J., Dai, J., Li, X.D., Liu, J.F., Chen, M., Lu, L.H., Hu, L., Wan, J., 2017. The interactions of composting and biochar and their implications for soil amendment and pollution remediation: a review. Crit. Rev. Biotechnol. 37, 754–764.
Xu, P., Zeng, G.M., Huang, D.L., Feng, C.L., Hu, S., Zhao, M.H., Lai, C., Wei, Z., Huang, C., Xie, G.X., Liu, Z.F., 2012a. Use of iron oxide nanomaterials in wastewater treatment: a review. Sci. Total Environ. 424, 1–10.
Xu, P., Zeng, G.M., Huang, D.L., Lai, C., Zhao, M.H., Wei, Z., Li, N.J., Huang, C., Xie, G.X., 2012b. Adsorption of Pb (II) by iron oxide nanoparticles immobilized *Phanerochate chrysosporium*. Chem. Eng. J. 203, 423–431.
Zeng, G.M., Zhang, L.H., Dong, H.R., Chen, Y.N., Zhang, J.C., Zhu, Y., Yuan, Y.J., Xie, Y.K., Fang, W., 2018. Pathway and mechanism of nitrogen transformation during composting: Functional enzymes and genes under different concentrations of PVP-AgNPs. Bioresour. Technol. 253, 112–120.
Zhang, C., Lai, C., Zeng, G.M., Huang, D.L., Yang, C.P., Wang, Y., Zhou, Y.Y., Cheng, M., 2016a. Efficacy of carbonaceous nanocomposites for sorbing ionizable antibiotic sulfamethazine from aqueous solution. Water Res. 95, 103–112.
Zhang, Y., Zeng, G.M., Tang, L., Chen, J., Zhu, Y., He, X.X., He, Y., 2015a. Electrochemical sensor based on electrodeposited graphene-Au modified electrode and nanoAu carrier amplified signal strategy for attomolar mercury detection. Anal. Chem. 87, 989–996.
Zhang, J.C., Zeng, G.M., Chen, Y.N., Yu, M., Yu, Z., Li, H., Yu, Y., Huang, H.L., 2011. Effects of physico-chemical parameters on the bacterial and fungal communities during agricultural waste composting. Bioresour. Technol. 102, 2950–2956.
Zhang, L.H., Zeng, G.M., Dong, H.R., Chen, Y.N., Zhang, J.C., Yan, M., Zhu, Y., Yuan, Y.J., Xie, Y.K., Huang, Z.Z., 2017. The impact of silver nanoparticles on the co-composting of sewage sludge and agricultural waste: evolutions of organic matter and nitrogen. Bioresour. Technol. 230, 132–139.
Zhang, L.H., Zeng, G.M., Zhang, J.C., Chen, Y.N., Yu, M., Lu, L.H., Li, H., Zhu, Y., Yuan, Y.J., Huang, A.Z., He, L., 2015b. Response of denitrifying genes coding for nitrite (*nirK* or *nirS*) and nitrous oxide (*nosZ*) reductases to different physico-chemical parameters during agricultural waste composting. Appl. Microbiol. Biot. 99, 4059–4070.
Zhang, Y.J., Li, H.C., Gu, J., Qian, X., Yin, Y.N., Li, Y., Zhang, R.R., Wang, X.J., 2016b. Effects of adding different surfactants on antibiotic resistance genes and *intl 1* during chicken manure composting. Bioresour. Technol. 219, 545–551.
Zhou, C.Y., Lai, C., Huang, D.L., Zeng, G.M., Zhang, C., Cheng, M., Hu, L., Wan, J., Xiong, W.P., Wen, M., Wen, X.F., Qin, L., 2018. Highly porous carbon nitride by supramolecular preassembly of monomers for photocatalytic removal of sulfamethazine under visible light driven. Appl. Catal. B-Environ. 220, 202–210.